Electronic supplementary information

MOF-derived Hexagonal In_2O_3 Microrods Decorated with $g\text{-}C_3N_4$ Ultrathin Nanosheets for Efficient Photocatalytic Hydrogen Production

Liujun Hu[&], Hongli Yang[&], Shuhua Wang, Junlun Gao, Huilin Hou[*] and Weiyou Yang[*]

Institute of Materials, Ningbo University of Technology, Ningbo, 315211, P. R. China

---

[&] These authors contributed equally to this work.

[*] Corresponding authors. E-mail: houhuilin86@163.com (H. Hou) and weiyouyang@tsinghua.org.cn (W. Yang)

Experimental

Materials

Urea, deionized water, indium nitrate ($In(NO_3)_3$), N,N-Dimethylformamide (DMF), sodium sulfide (Na_2S), terephthalic acid (BDC), sodium sulfate (Na_2SO_4), commercial In_2O_3, and sodium sulfite (Na_2SO_3) were provided by Aladdin and Titan. These reagents were utilized as received without any additional purification.

Preparation of In_2O_3@g-C_3N_4 heterojunction photocatalyst

The fabrication process of the In_2O_3@g-C_3N_4 heterojunction is shown in Figure 1. The thermopolymerization reaction was initially employed to synthesize the g-C_3N_4 nanosheets. In this process, 5 g of urea was ground into fine powders, which was later added to a covered crucible and heated for 2 h within the muffle furnace at 500°C. Simultaneously, 120 mg $In(NO_3)$ and 120 mg BDC were dissolved in 80 ml DMF to form a mixed solution. Subsequently, 150 mg of the obtained g-C_3N_4 nanosheets were dispersed in the mixed solution under vigorous stirring for 5 h. Thereafter, the obtained suspension was transferred into an oil bath device. For the preparation of g-C_3N_4/In-MOFs, the temperature of the oil bath was set to 120 °C. Finally, the obtained g-C_3N_4/In-MOFs were heated in a muffle furnace. During this process, the heating rate, target temperature, and maintained time were 5 °C min^{-1}, 500 °C, and 2 h, respectively. The In-MOF-derived In_2O_3 nanorods were comparatively studied. In comparison, the common In_2O_3@g-C_3N_4 heterojunction photocatalyst were also prepared trough grinding the mixture of g-C_3N_4 nanosheets and commercial In_2O_3 followed by an annealing process.

Characterization

The field emission scanning electron microscopy (FESEM, S-4800, Hitachi, Japan) was conducted for the systemic characterization of the samples. In addition, the X-ray powder diffraction (XRD, D8 Advance, Bruker, Germany) was used to analyze the phase structure by adopting the Cu Kα radiation (λ= 1.5406 Å). The structure and morphology of the samples were studied using energy-dispersive X-ray spectroscopy (EDX, Quantax-STEM, Bruker, Germany) and transmission electron microscopy

(TEM, JEM-2010F, JEOL, Japan), respectively. Moreover, XPS (ES-CALAB 250Xi, ThermoFisher Scientific, America) was utilized to measure the chemical states and surface species. The UV-visible spectrophotometer (UV-3900, Hitachi, Japan) was also adopted for recording the diffuse reflectance absorption spectra of the product using the composite sphere attachment. Photoluminescence spectra (PL) were recorded at room temperature using a fluorescence spectrophotometer (Fluromax-4P, Horiba Jobin Yvon, France).

Measurement of Photocatalytic Activity

The inner-irradiation quartz annular reactor was used for the photocatalytic evolution of H_2 by the irradiation of the samples with UV-vis light. Additionally, a 300W Xenon lamp (CEL, HUL300) was used as the source of light. Other components included a gas collector, vacuum pump (Vacuumize), water-cooled condenser, and recirculation pump. Thereafter, 0.1 g of the prepared products were dispersed in 40 mL of deionized water, and then 10 ml of Na_2S and Na_2SO_3 mixed solutions (0.5 M) were added to the aqueous solution through the ultrasonic oscillator. Thereafter, the mixed product was placed in the quartz reactor, which was deaerated using the vacuum pump and purged with N_2 for 30 min in order to remove gas. Finally, the Xenon lamp with a fixed light power density of 100 mW/cm^2 was employed to irradiate the photoinduced water splitting process. During the photocatalytic reaction, the temperature was kept under 25°C by passing through cold water. Additionally, the online gas chromatography (GC, 7900) was used to monitor the hydrogen content with the help of a thermal conductivity detector (TCD).

Photoelectrochemical measurements

To study the photoelectrochemical performance, the photoelectrodes were initially fabricated. The slurry was prepared by grounding a mixture of 0.1 g of sample products and 0.8 g of ethanol. Then, the drop method was employed to coat the slurry onto an indium-tin oxide (FTO) glass. Afterward, the FTO coated with the slurry was dried in a vacuum oven and further calcined at 200°C for 30 min to enhance the interface bonding. The photoelectrochemical performance of the sample products was studied using a standard three-electrode system consisting of an electrochemical analyzer (CHI 760e Instruments, Shanghai, China), Pt counter electrode, working electrode, and Ag/AgCl reference electrode. The intensity of the A300W Xenon lamp (CEL, HUL300) light source was fixed at 100 mW/cm^2. In addition, the Na_2SO_4 solution (0.5 M) was adopted as the electrolyte.

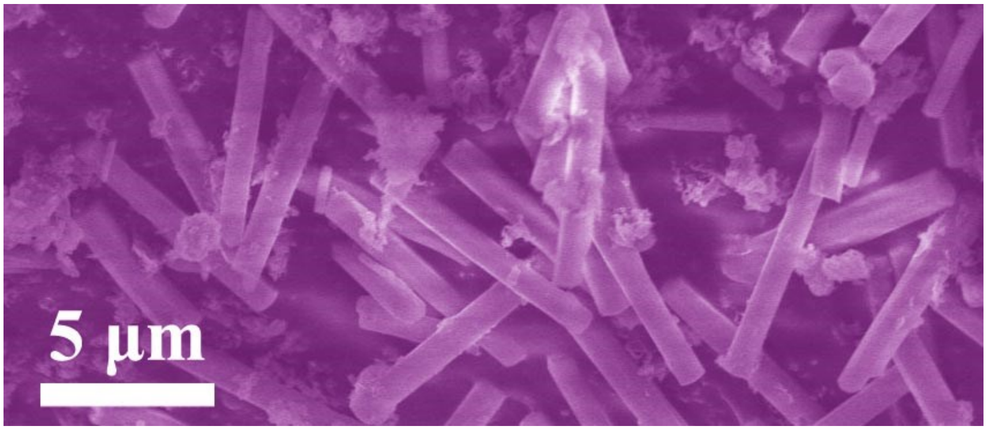

Fig. S1. A typical SEM image of as-prepared MOFs@g-C_3N_4 sample.

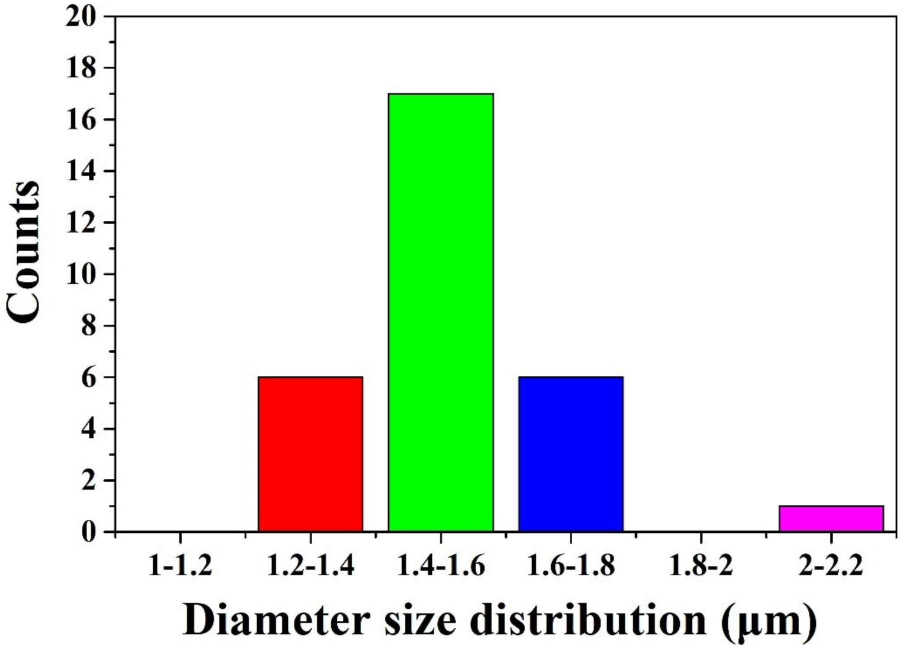

Fig. S2. Dimensional distribution of In_2O_3 microrods

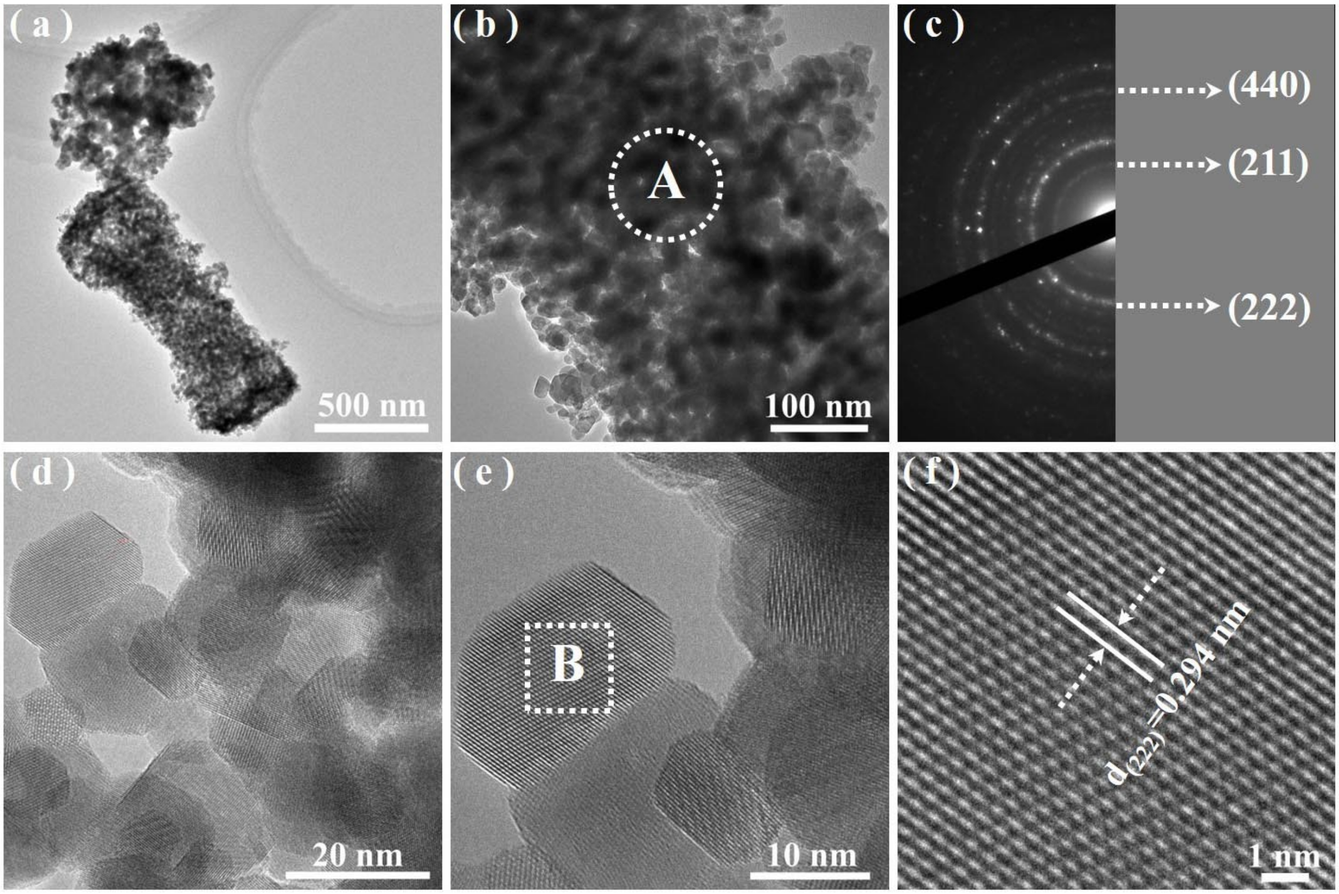

Fig. S3. (a-b) TEM images of the as-prepared In_2O_3 microrods under different magnifications. (c) SAED pattern from the marked area A in (b). (d-e) Representative HRTEM images. (f) An enlarged image of the the marked area B in (e).

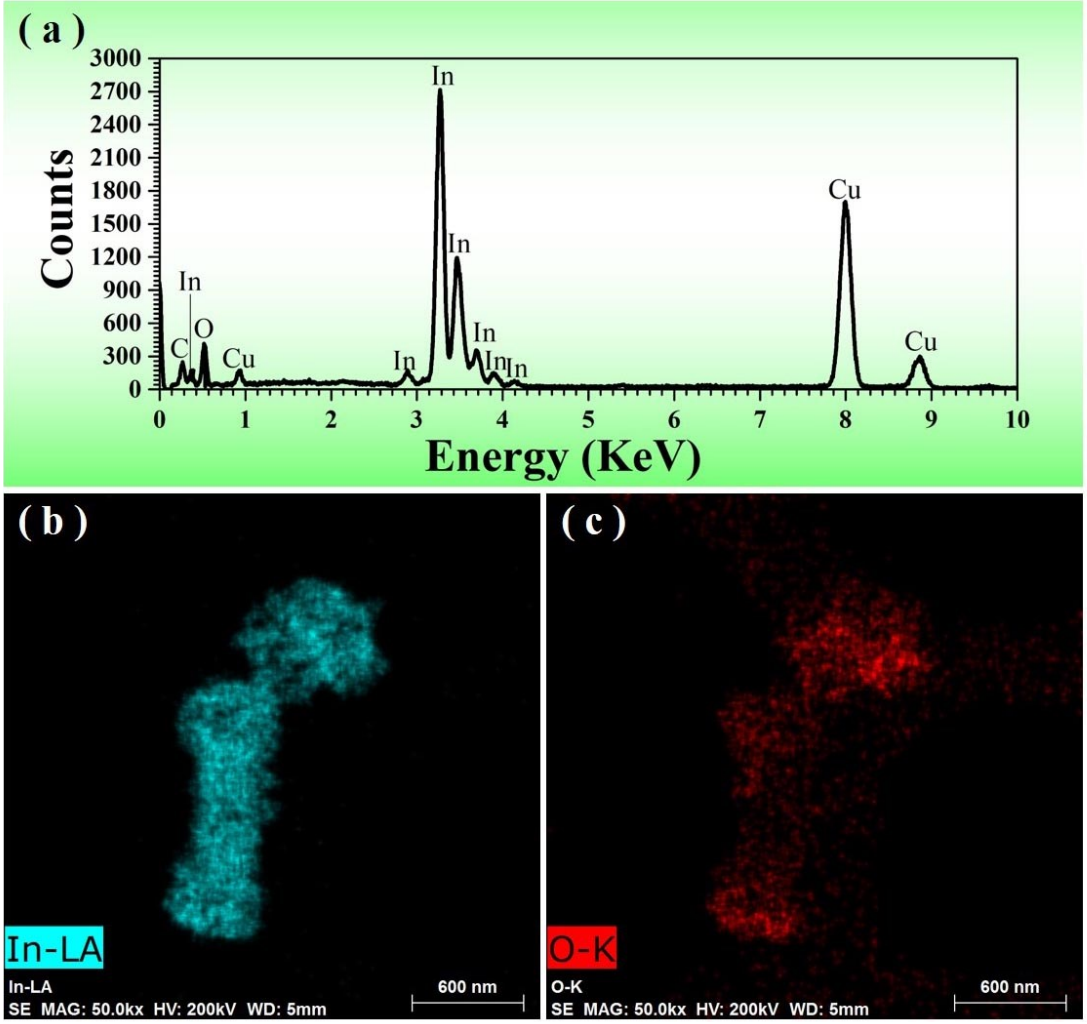

Fig. S4. (a) EDS spectrum of the as-prepared In_2O_3 microrods. (b-c) The EDS element mappings (In and O, respectively) of In_2O_3.

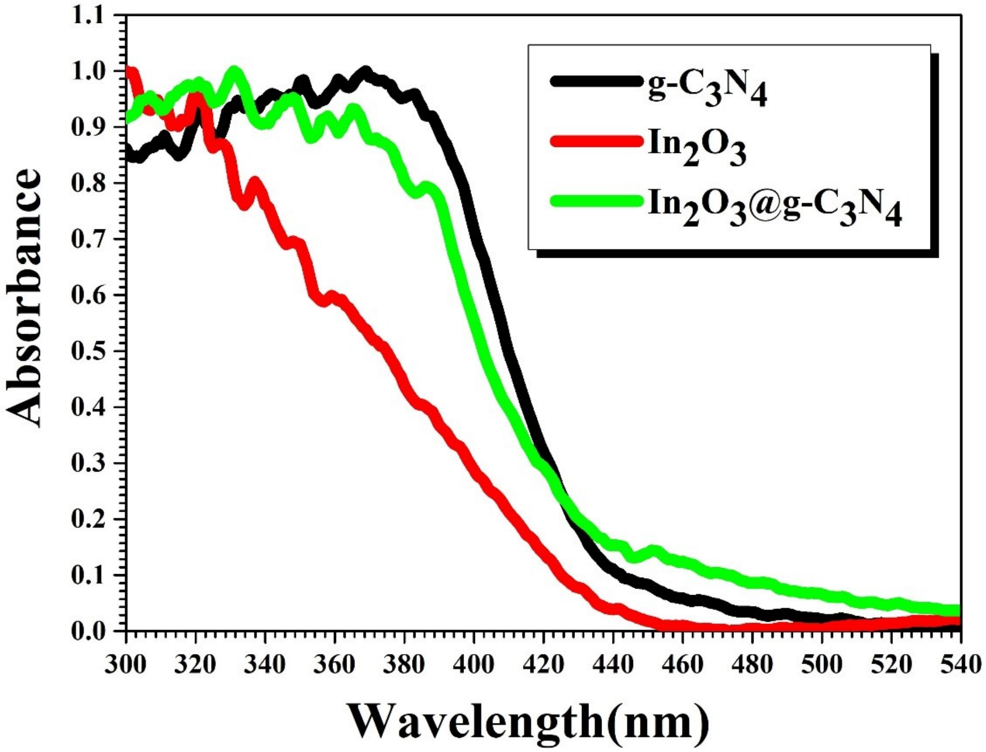

Fig. S5. UV-vis diffuse reflectance spectra of g-C_3N_4 nanosheets, MOFs-derived In_2O_3 and In_2O_3@g-C_3N_4 heterojunction.

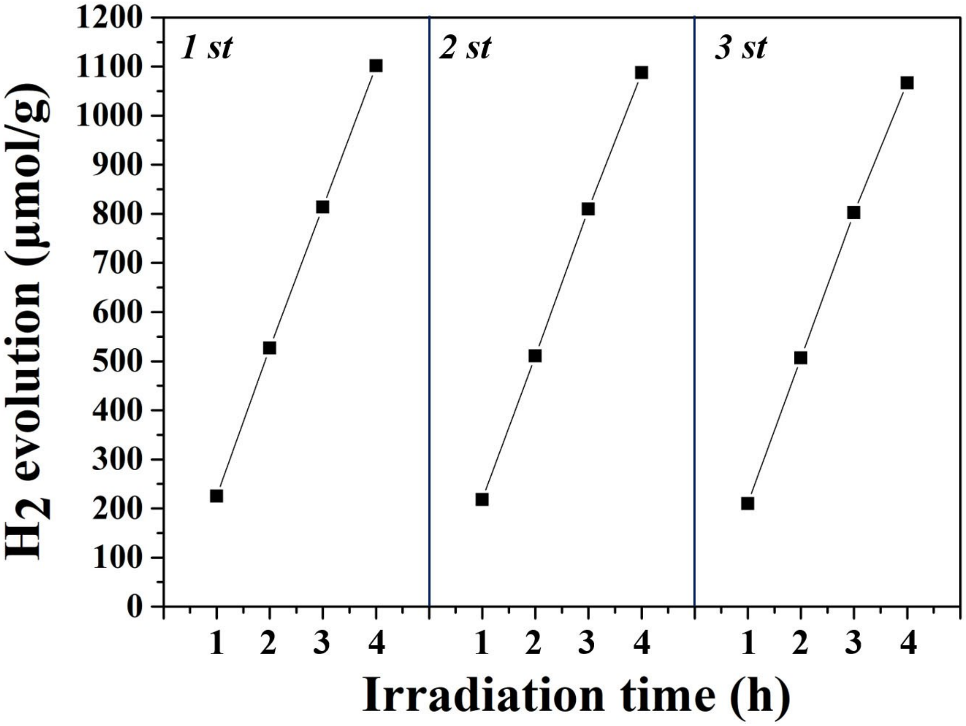

Fig. S6. Cycling tests over In_2O_3@g-C_3N_4 sample photocatalyst.

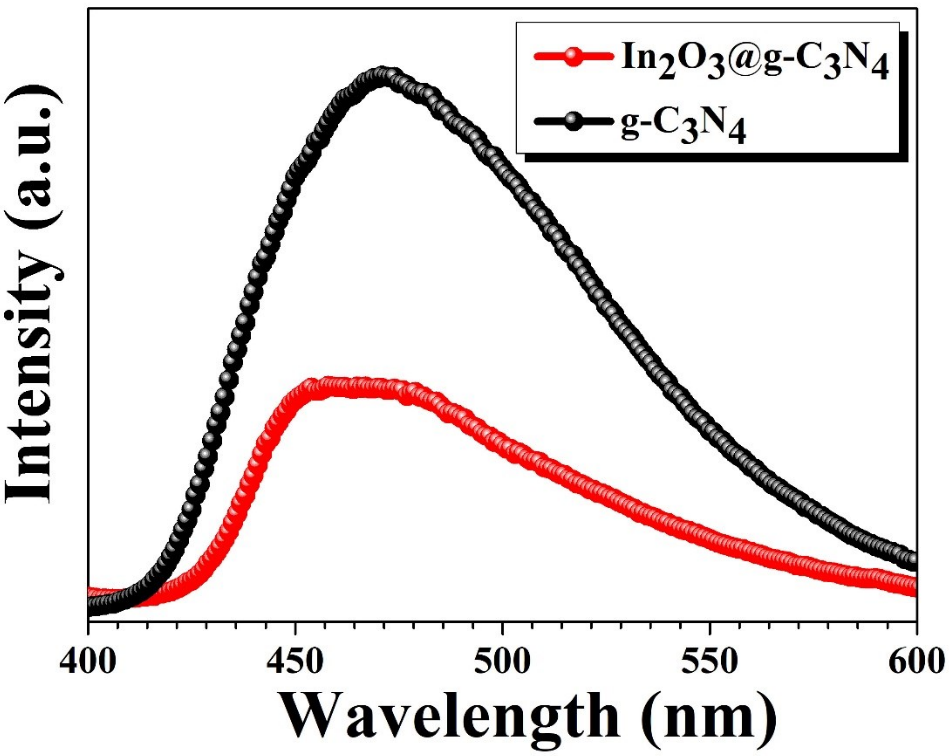

Fig. S7. PL spectra of g-C_3N_4 and In_2O_3@g-C_3N_4 samples.

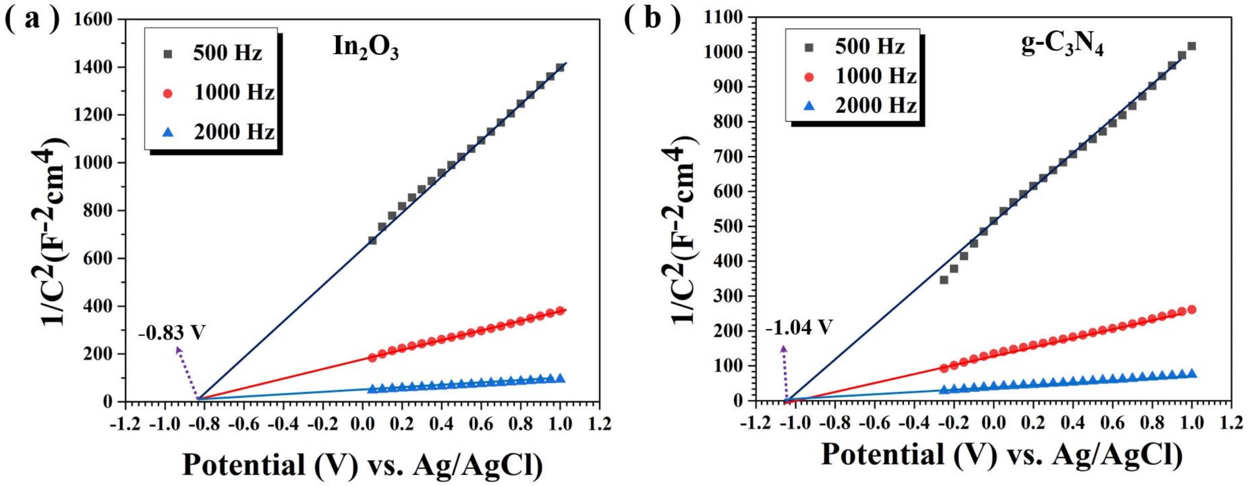

Fig. S8. Mott-Schottky plots of In_2O_3 (a) and g-C_3N_4 (b) samples measured at t at frequencies of 500, 1000 and 2000 Hz.

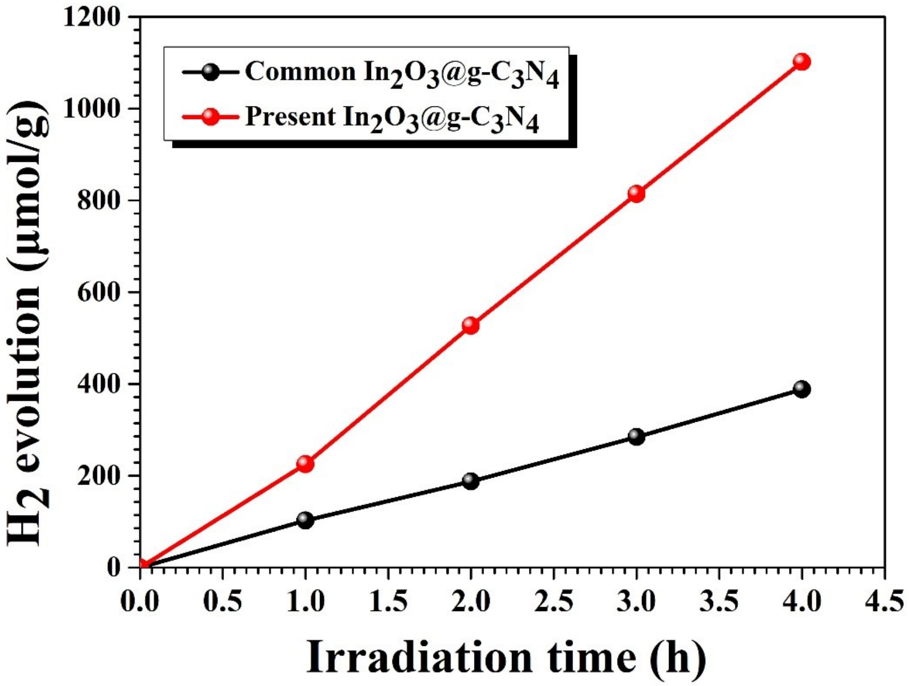

Fig. S9. Comparison of the photocatalytic H_2 evolution activity with the common In_2O_3@g-C_3N_4 photocatalysts

Table S1. Comparison of the reported In_2O_3 based photocatalysts for photocatalytic H_2 production

Material	Cocatalyst	Irradiation conditions	Sacrificial agent	Activity (μmol g^{-1}h^{-1})	Reference
In_2O_3/Ta_2O_5	Pt	300 W xenon lamp	Methanol	189	1
Gd_2Ti_2O7/In_2O_3	---	300 W xenon lamp	Methanol	289.9	2
$In_2O_3/La_2Ti_2O_7$	---	500 W Xe lamp	Methanol	68.14	3
In_2O_3@g-C_3N_4	Pt	300 W xenon lamp	L-ascorbic acid	197.5	4
$In_2S_3/CdIn_2S_4/In_2O_3$	Pt	225 W xenon arc lamp	Na_2SO_3+Na_2S	200.4	5
CdS/ In_2O_3	---	300 W xenon lamp	Triethanolamine	235.05	6
In_2O_3-In_2S_3	---	300 W xenon lamp	Triethanolamine	136.75	7
In_2O_3/S-doped g-C3N4	---	300 W xenon lamp	Triethanolamine	91.7	8
In_2O_3@g-C_3N_4	Pt	300 W xenon lamp	Triethanolamine	68.4	9
In_2O_3@g-C_3N_4	---	300 W xenon lamp	Na_2SO_3+Na_2S	258.8	This work

References

1. L. Xu, J. Guan, L. Gao and Z. J. C. C. Sun, *Catal. Commun.*, 2011, **12**, 548-552.

2. A. Nashim , S. Martha and K. M. Parida, *ChemCatChem*, 2013, **5**, 2352-2359.

3. S. Hu, B. Chi, J. Pu and L. J. J. o. M. C. A. Jian, *J. Mater. Chem. A*, 2014, **2**, 19260-19267.

4. S.-W. Cao, X.-F. Liu, Y.-P. Yuan, Z.-Y. Zhang, Y.-S. Liao, J. Fang, S. C. J. Loo, T. C. Sum and C. Xue, *Appl. Catal. B*, 2014, **147**, 940-946.

5. D. Ma, J. W. Shi, Y. Zou, Z. Fan, J. Shi, L. Cheng, D. Sun, Z. Wang and C. Niu, *Nanoscale*, 2018, **10**, 7860-7870.

6. J.-T. Ren, K. Yuan, K. Wu, L. Zhou and Y.-W. Zhang, *Inorg. Chem. Front.*, 2019, **6**, 366-375.

7. M. Liu, P. Li, S. Wang, Y. Liu, J. Zhang, L. Chen, J. Wang, Y. Liu, Q. Shen, P. Qu and H. Sun, *J.*

Colloid Interface Sci., 2020, DOI: 10.1016/j.jcis.2020.11.048.

8. P. Zhou, X. Meng and T. Sun, *Mater. Lett.*, 2020, **261,** 127159.

9. X. Liu, L. Zhang, Y. Li, X. Xu, Y. Du, Y. Jiang and K. Lin, *Mater. Res. Bull.*, 2021, **133,** 111078.